Systematic study of the photodisintegration of ^{70}Ge, ^{72}Ge, ^{74}Ge, and ^{76}Ge

J. J. McCarthy,* R. C. Morrison,† and H. J. Vander Molen‡
Ames Laboratory-USAEC and Department of Physics, Iowa State University, Ames, Iowa 50010
(Received 28 May 1974)

Cross sections for the (γ, n), the $(\gamma, 2n)$, and the (γ, np) reactions for ^{70}Ge, ^{72}Ge, ^{74}Ge, and ^{76}Ge, and the (γ, p) reaction for ^{74}Ge have been measured from threshold to 40 MeV at the Iowa State University Synchrotron Laboratory. Cross section results were obtained by unfolding bremsstrahlung yield curves. A "total" photoabsorption cross section was obtained for each isotope by adding the partial cross sections together. Cross sections integrated to 40 MeV are given for each reaction. Giant resonance parameters obtained from the total cross sections are compared with the results of a dynamic collective model calculation. Cross section strength is found at energies above the giant dipole resonance and is discussed in terms of the integrated cross sections.

[NUCLEAR REACTIONS ^{70,72,74,76}Ge(γ, n), $(\gamma, 2n)$, $E_\gamma = 9$–40 MeV; measured $\sigma(E\gamma)$. Enriched targets. ^{70,76}Ge(γ, n), ^{70,72,74,76}Ge(γ, np), ^{74}Ge(γ, p), $E = 9$–40 MeV; measured $\sigma(E\gamma)$. Natural targets. Total σ's compared with dynamic collective model.]

I. INTRODUCTION

The electric dipole resonance observed in the photodisintegration of all nuclei has been intensively studied for many years. The systematics of the photoabsorption cross section have been of interest since the discovery of the giant resonance. At the present time, models of nuclear structure provide a fairly detailed description of photoabsorption and the giant resonance. It is our intention in this work to carry out a systematic comparison between the predictions of the dynamic collective theory of photoabsorption and a set of experimental measurements recently performed at this laboratory.

In the middle of the last decade Danos and Greiner,[1] Le Tourneux,[2] Semenko,[3] and Kerman and Quang[4] pointed out that the quadrupole oscillations of the nuclear surface could couple to the giant dipole resonance oscillation to produce added complexity in the structure of the giant resonance. This model, called the dynamic collective model, predicts the giant resonance will be split into several peaks for most nuclei. The magnitude of these effects depends upon the "softness" of the nuclear surface which can be characterized by the nuclear deformation and the energy of the low lying collective states. The predicted energies of this structure in the giant resonance agree quite well with experimental results,[5,6] even for as light a nucleus as ^{75}As, but the calculated strengths often disagree with experimental data.

The existence of an appreciable cross section for photonuclear interactions at energies well above the giant resonance has been inferred in many instances because of the failure of the integrated cross section in the giant resonance region to exhaust the dipole sum.[7,8] Danos[9] has suggested the existence of electric giant quadrupole and dipole overtone resonances on the basis of a hydrodynamic model of the nucleus. More recently, Ligensa and Greiner[10] have calculated the size and shape of the giant quadrupole resonance using a more sophisticated collective model. This result seems to be confirmed in experimental results by groups at Livermore[11] and Saclay.[12] The energies of these electric quadrupole transitions fall above the giant dipole resonance in most instances.

Since many models predict a systematic dependence of the giant resonance properties upon parameters such as the nuclear mass, charge, shape, and excitation energy, it is desirable to design experimental studies to test the gross dependence of the giant resonance on one or more of these model parameters. The present study of germanium isotopes is intended to serve such a purpose. In terms of the dynamic collective calculations of the interaction of the dipole and quadrupole vibrations, the germanium nuclei are of considerable interest. The characteristics of the low-lying vibrational levels which enter into the dynamic collective description of the giant resonance imply a systematic spreading of the main dipole state with the smallest width for the ^{70}Ge giant resonance, and the largest width for ^{76}Ge. This spreading should be easy to detect in an experiment and can provide a good test of dynamic collective theory in this mass region. In order to perform such a test we have measured the major photodisintegration cross sections of four germanium isotopes in two separate experiments at this

laboratory. The measurements were extended to 40 MeV in order to obtain an estimate of the cross section present at excitation energies above the giant dipole resonance.

II. APPARATUS AND PROCEDURE

Two separate experiments were carried out at the Iowa State University Synchrotron Laboratory to measure the cross sections reported here. In both experiments cross sections were unfolded from bremsstrahlung yield curves. In the first experiment, (γ, n) and $(\gamma, 2n)$ cross sections for ^{70}Ge, ^{72}Ge, ^{74}Ge, and ^{76}Ge were measured by direct neutron detection using targets of isotopically separated germanium metal. The photoneutrons emitted during bombardment were counted in 4π geometry by a high-efficiency neutron-sensitive scintillation detector. In the second experiment, the (γ, n) cross section of ^{70}Ge and ^{76}Ge, the (γ, p) cross section of ^{74}Ge, and the (γ, np) cross sections of ^{70}Ge, ^{72}Ge, ^{74}Ge, and ^{76}Ge were measured by counting residual activity following activation of targets of natural germanium metal by bremsstrahlung. The residual nuclei populated by all the (γ, np) reactions, the (γ, p) reaction of ^{74}Ge, and the (γ, n) reactions of ^{70}Ge and ^{76}Ge are β emitters and have associated characteristic γ-ray transitions. The specific reaction end products were identified by counting the activated samples in a Ge(Li) γ-ray spectrometer.

Since the (γ, n) cross sections of ^{70}Ge and ^{76}Ge were measured in both experiments, they provide a check on the absolute calibrations of the two measurements. The close agreement of the two results enables a direct addition of the partial cross sections from different experiments for the synthesis of total photodisintegration cross sections.

A. Neutron counting experiment

The experimental arrangement is shown in Fig. 1. Bremsstrahlung from the internal synchrotron radiator passed through two collimators prior to passing through an evacuated beam tube in the detector. The germanium target was located in the center of the detector, and was centered on the axis of the photon beam. After leaving the detector shielding house, the photon beam was incident on a calibrated ionization chamber. The scintillation monitor shown in Fig. 1 was slightly off axis and was used to detect the "beam flash" of the synchrotron to act as a time base for the counting cycle.

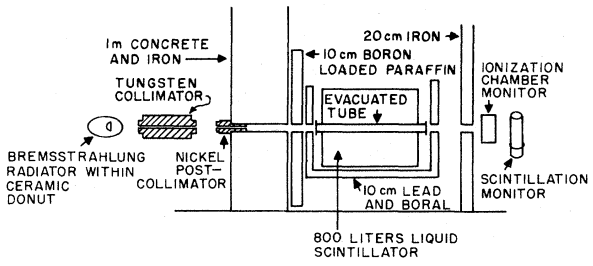

FIG. 1. Experimental arrangement for direct photoneutron detection.

The neutron detector used in this experiment was a cylindrical tank, 1.0 m in diameter and 1.1 m in length, containing approximately 800 liters of petroleum-based liquid scintillator loaded with 5 kg of gadolinium and viewed by 28 photomultipliers.

The counting efficiency of the detector was determined with a weak ^{252}Cf fission source. The source was mounted between two surface barrier fission fragment detectors, and placed at the target position in the center of the detector's beam tube. The detector timing cycle was initiated by the surface barrier detectors, and the number of counts per fission measured. Since the average number of neutrons per fission is known[13] to be 3.725 ($\pm$0.5%), the detector efficiency could be directly calculated. Over the entire experiment, the observed efficiency was 73.6% $\pm$ 0.5%.

Data runs lasted one hour and were taken at beam energies from 10 to 40 MeV in 2 MeV steps. The detector was gated off for 2 μsec as the beam pulse (1 μsec duration) passed through. The detector then was gated on for 20 μsec to count neutrons. After a wait of 6 msec, the detector was gated on again for 100 20-μsec intervals to record background counts. Neutron data counts were analyzed into channels called multiplicity bins. If a beam burst produced no neutron counts at all, bin zero was incremented. If one neutron was detected, bin one was incremented, if two were detected, bin two was incremented, and so on. These data were later statistically analyzed to extract the reaction rates for the (γ, n) and $(\gamma, 2n)$ reactions. A complete yield curve contained 16 different bremsstrahlung energies. The various energies were run in random order until at least three yield points at each energy were obtained.

The measurement of the (γ, n) and $(\gamma, 2n)$ cross sections required targets of isotopically separated germanium. Separated isotopes of germanium were obtained from Oak Ridge National Laboratory in the form of GeO. In order to avoid contamination of the yield data with the effects of oxygen resonances, the GeO samples were reduced to metallic germanium. The targets were fabricated into wafers with a beam interception area of about 1.5 cm^2 and average weight of 0.98 g. The isotopic purity of each sample is shown in Table I.

TABLE I. Target parameters for neutron counting experiment.

Isotope	Mass (g)	^{70}Ge (%)	^{72}Ge (%)	^{73}Ge (%)	^{74}Ge (%)	^{76}Ge (%)
^{70}Ge	0.9774	98.8	0.71	0.10	0.29	0.10
^{72}Ge	0.9766	2.70	90.88	1.27	4.23	0.93
^{74}Ge	0.9860	1.27	1.61	0.64	95.98	0.51
^{76}Ge	0.9893	7.69	6.65	1.69	10.08	73.89

B. Activation experiment

The experimental arrangement for the activation work is shown in Fig. 2. In this measurement, bremsstrahlung was used to irradiate targets of natural germanium. Immediately after leaving the accelerator, the photon beam entered the primary collimator. The germanium target was placed in a holder on the end of this collimator. The beam passed through the target, through a hole in the 100 cm thick shielding wall, and struck the beam monitor. The diameter of the collimated beam at the sample position was 2.2 cm, which was smaller than the diameter of the germanium samples. After irradiation, samples were removed from the accelerator room to be counted in the γ-ray spectrometers.

The germanium samples used in the activation experiment were discs of natural germanium of average weight 16 g with average diameter 2.9 cm and thickness 0.5 cm. Thirty-six samples were used to allow enough time for long-lived activities to decay away between successive activations.

Two different photon spectrometers were used to record the γ-ray spectra of the activated germanium samples. Each spectrometer consisted of a high efficiency Ge(Li) detector and a 512 Channel analog-to-digital converter (ADC) interfaced to an on-line computer. Detector pulses were amplified, shaped, and then routed to an ADC. During each counting period a γ spectrum for the activated sample was collected in the computer memory. These spectra were analyzed off-line to provide yield points.

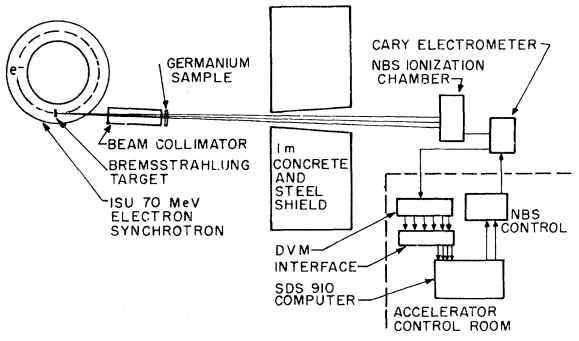

FIG. 2. Experimental arrangement for activation measurements.

The spectrometers were calibrated in terms of γ-ray energy using standard γ sources. Prior to the experiment, every γ ray in the spectra of activated samples was identified by energy and half-life.

The absolute efficiency and energy resolution of each detector were measured directly using calibrated standard sources. Both systems had energy resolutions of better than 3.5 keV and absolute efficiencies of $1.086\% \pm 0.012\%$ and $0.76\% \pm 0.006\%$, respectively, at 1.33 MeV.

Yield curves for all reactions were measured simultaneously in 1 MeV energy steps from 9 to 40 MeV. The bremsstrahlung end-point energy was varied randomly to minimize any time-dependent systematic error. At least four yield points were measured at each energy. Samples were precounted before irradiation to determine background and residual activity from previous activations. The sample was then irradiated with bremsstrahlung, transferred to the spectrometer, and counted. The on-line computer supervised experimental timing and calculated crude yields as a check on experimental progress.

III. TREATMENT OF DATA

A. Yield curves obtained from direct neutron detection

The multiplicity-bin analysis of the neutron counts for each individual beam burst allowed the statistical extraction of the reaction multiplicities. Since this experiment covered energies up to and including 40 MeV, it was energetically possible to have emission of up to four neutrons. The form of the multiplicity spectrum and the reaction rates were calculated using the algorithm for nonlinear regression of Marquardt[14] and Bevington.[15] Initial estimates for the reaction rates were computed using Goryachev's method.[16]

Once the reaction rates for the four energetically allowed reactions were extracted from the data, the reaction yields could be calculated. The reaction rates were divided by beam monitor response to form uncorrected yields. The final (or reduced) yields were calculated by the application of an energy-dependent correction for the response of the beam monitor to the bremsstrahlung beam. Attempts to extract yield curves for $(\gamma, 3n)$ and $(\gamma, 4n)$ reactions were unsuccessful because of relatively large errors encountered in the multiplicity analysis.

After the reduced yield from each bombardment was calculated, the beam-induced background

yields were averaged together and subtracted from the data yields. The differences, which were the yields from the germanium target, were averaged to give one reduced yield curve for each of the (γ, n) and $(\gamma, 2n)$ reactions. Error estimates for the reduced yields were calculated from the spread of the unaveraged yields at each end-point energy.

Yield curves from 10 to 40 MeV were obtained in this fashion for the reactions ^{70}Ge(γ, n), ^{70}Ge$(\gamma, 2n)$, ^{72}Ge(γ, n), ^{72}Ge$(\gamma, 2n)$, ^{74}Ge(γ, n), ^{74}Ge$(\gamma, 2n)$, ^{76}Ge(γ, n), and ^{76}Ge$(\gamma, 2n)$.

B. Yield curves obtained from residual radioactivity measurements

Since the raw data from the activation measurement were recorded as a series of γ-ray spectra containing peaks from all activities of interest, a computer code was devised to locate desired peaks, obtain the area of each peak, and correct for the response of the beam monitor. The area of each peak was calculated by numerical integration after fitting and subtracting off the background spectrum. These areas were divided by the beam monitor response to form the reduced yields. This portion of the measurement provided yield curves for the reactions ^{70}Ge(γ, n), ^{70}Ge(γ, np), ^{72}Ge(γ, np), ^{74}Ge(γ, p), ^{74}Ge(γ, np), ^{76}Ge(γ, n), and ^{76}Ge(γ, np).

C. Extraction of cross section results

Cross sections were obtained from the reduced yields using the "least structure" method developed at this laboratory by Cook.[17] In this method, the smoothest cross section statistically consistent with the reduced yields and their uncertainties is calculated. This technique has been critically analyzed and compared with other methods by Bramanis *et al.*[18] Since the smoothing implicit in the least structure method could conceivably give rise to false structure in the cross section, it is essential that this aspect of the data reduction be most carefully monitored. The computer codes used to extract cross sections from the yield data also produce resolution functions and cross section error estimates. Use of these resolution functions, along with checks for internal consistency such as trial analyses with truncated data sets, allows the extraction of reliable cross sections using the "Least Structure" technique. Typical resolution functions obtained by unfolding the yield data of this experiment are shown in Fig. 3. Each resolution function curve shows the shape that would appear in the extracted cross section for a δ-function resonance in the true cross section. Some "overshoot" is apparent in these resolution functions, reflecting the statistical quality of the yield data. The resultant oscillations damp out quite quickly but are large enough to alter the shape of the cross section, particularly in regions where the cross section is small. In the case of the worst statistical data, as we shall point out in the following, the overshoot is large enough to distort the cross section results to some degree.

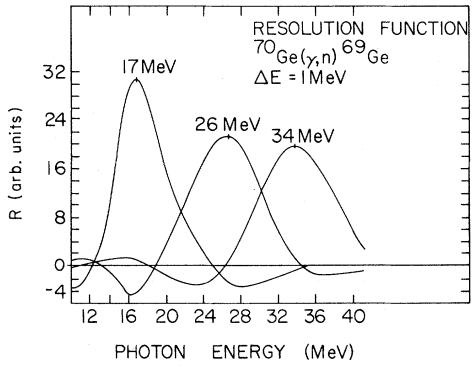

FIG. 3. Typical "resolution functions" for cross sections obtained in this measurement.

In addition to resolution functions the analysis provides a highly correlated sequence of error estimates, one for each cross-section point. Since smoothing establishes a high degree of successive point correlation in the cross-section result, smooth curves should be drawn through the point sequence rather than just within the error bars. For these reasons, error bars are provided only at intervals in the plotted results to demonstrate the error trend. The vertical error bars reflect the total statistical uncertainty in the cross-section points. The horizontal bars above the curve are not uncertainties in the energy. Rather, they are to be associated with the corresponding resolution function for the cross section at this point. If the true physical cross section had the form of a δ function, the least structure analysis would produce a smoothed resonance with a full width at half-maximum (FWHM) equal to the horizontal error bar.

Cross section normalizations were calculated by determining the number of incident photons on the target, and other quantities peculiar to the geometry of each of the experiments. For the neutron counting results the normalization between isotopes was determined to better than 0.5%. The presence of isotopic impurities in the targets introduces an additional uncertainty of about 3% into the cross-section scales. Statistical uncertainties in the unfolded cross sections averaged 15% for the (γ, n) results at the peak of the giant resonance, and 26% for the $(\gamma, 2n)$ results at the cross-section peak value. The total estimated uncertainty in the absolute normalization of the neutron cross sections is 20%. In the activation results the greatest

uncertainty in the normalization is due to the uncertainties in the branching ratios of the γ transitions used to calculate the yields. The total uncertainty in these normalizations is estimated to be about 15%. Statistical uncertainties average to 8% at the peak of the giant resonance for the activation results.

Above the giant resonance, the statistical uncertainties propagated by the unfolding procedure increase considerably. These large uncertainties, combined with the poor resolution above 25 MeV as obtained from the resolution functions, indicates that the cross-section shapes at higher energies are not reliable. The integrated cross sections are not subject to these uncertainties, and are accurate to within the statistical uncertainty of the yield data.

IV. RESULTS

The intention of these experiments was to investigate the gross systematics of the photodisintegration of several germanium isotopes. Accordingly, yield points were widely spaced in energy with the result that the final cross sections appear in poor resolution. For this reason, exact agreement with threshold energies and the like is not expected and will not be emphasized in the discussion of cross-section data. The cross-section data for ^{70}Ge, ^{72}Ge, ^{74}Ge, and ^{76}Ge are presented in Figs. 4 through 7, respectively. Each figure presents the (γ, n), $(\gamma, 2n)$, and total $[(\gamma, n) + (\gamma, np) + (\gamma, 2n) + (\gamma, p)]$ cross section for each isotope. The integrated cross section data are presented in Table II.

The ^{70}Ge(γ, n) cross section and the ^{76}Ge(γ, n) cross section were measured by both the activation and neutron counting experiments. In both cases, the activation yield data were of better statistical quality (average yield uncertainty of ±8% for ^{70}Ge, ±4% for ^{76}Ge) than the neutron counting yield data (average yield uncertainty of ±20% for ^{70}Ge, and ±14% for ^{76}Ge) and therefore the (γ, n) cross sections presented here are the activation results.

The yield data for these reactions from both experiments were in agreement within the statistical uncertainties of the neutron counting data at each yield point. This agreement has allowed us to add together the partial cross sections measured in the two experiments to construct total cross sections without applying further normalizations to either the activation or neutron counting results.

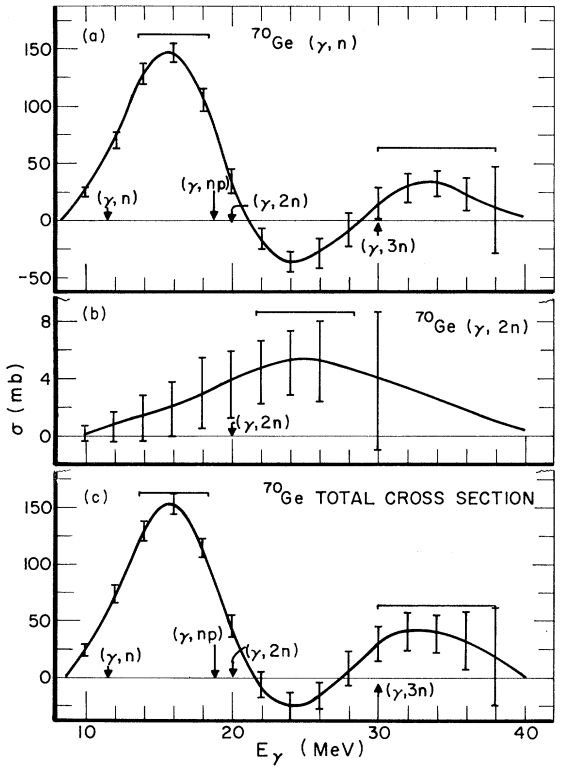

FIG. 4. (a) The (γ, n) cross section for ^{70}Ge. (b) The $(\gamma, 2n)$ cross section for ^{70}Ge. (c) The total cross section $\sigma[(\gamma, n) + (\gamma, 2n) + (\gamma, np) + (\gamma, p)]$ for ^{70}Ge. The thresholds (arrows) are taken from Ref. 26.

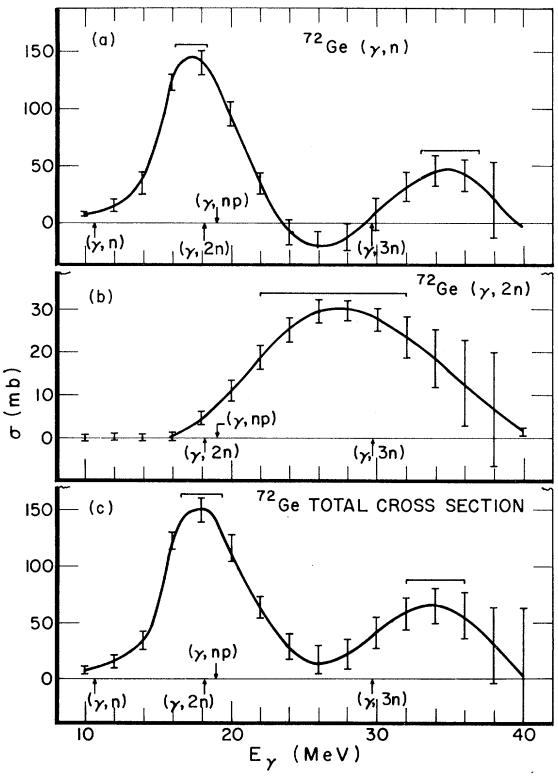

FIG. 5. The (γ, n) cross section for ^{72}Ge. (b) The $(\gamma, 2n)$ cross section for ^{72}Ge. (c) The total cross section $\sigma[(\gamma, n) + (\gamma, 2n) + (\gamma, np) + (\gamma, p)]$ for ^{72}Ge.

TABLE II. Integrated cross sections.

Isotope	(γ,n)	$(\gamma,2n)$	(γ,p) (MeV mb)	(γ,np)	Total
^{70}Ge	1273(127) [a] 1464(290) [b]	60(6)		40(6)	1463(128)
^{72}Ge	1140(110)	420(40)		40(14)	1690(118)
^{74}Ge	1320(130)	360(40)	90(10)	35(3) [c]	1805(136)
^{76}Ge	1077(54) [a] 1067(106) [b]	710(70)		15(3)	1892(89)

[a] Result of the activation measurements.
[b] Result of the neutron counting measurements.
[c] Includes the contribution from the ^{73}Ge(γ,p) reaction.

In preparing the total cross section curves we have adopted the following procedures. The partial reaction cross sections for each major decay channel have been added together to obtain the "total" contribution at each energy. In the case of ^{70}Ge and ^{72}Ge, the negative cross section above the giant resonance has been included in the sum. The (γ,p) and (γ,np) data, measured by the activation experiment, have been reported previously,[19] and are not presented explicitly here. However, they have been included in the total cross-section results.

The ^{74}Ge(γ,p) cross section was the only (γ,p) result obtained and has been used to estimate the (γ,p) contribution to the total cross section in ^{70}Ge, ^{72}Ge, and ^{76}Ge. This substitution is likely to introduce some error into the total integrated cross section. While the $^{74}(\gamma,p)$ reaction is less than 10% of the integrated cross section for the ^{74}Ge(γ,n) reaction, the ratio of (γ,p) to (γ,n) can be expected to vary for neighboring Ge isotopes, since the proton threshold energies vary by as much as 4 MeV. This same shift in threshold energy produces a factor of 10 change in the $(\gamma,2n)$ results.

A. Cross-section data

1. ^{70}Ge

The ^{70}Ge data have the largest statistical uncertainties of all the activation results. In the case of the single neutron data, this is due mainly to the very long-lived activity (40 h) of the daughter nucleus. As a result, some distortion of the (γ,n) cross section is introduced by the unfolding analysis in the regions where the cross section is small and the statistical uncertainties are large. This distortion appears in the cross section in two

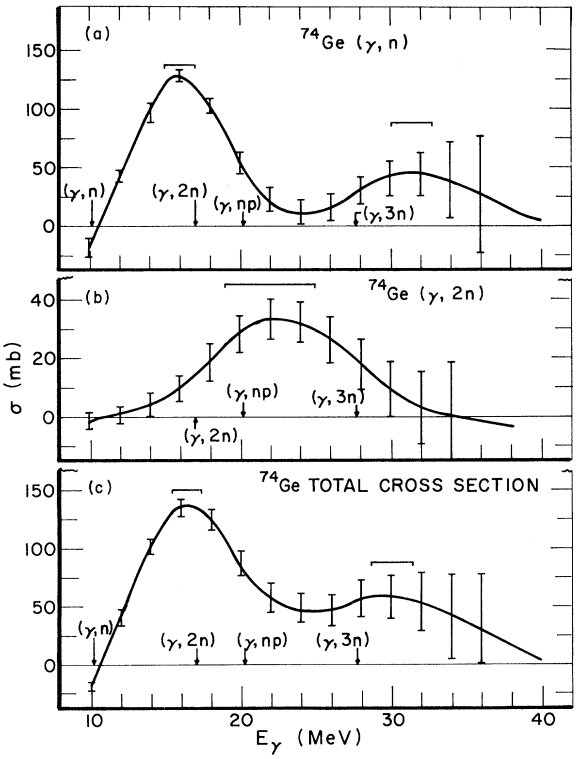

FIG. 6. (a) The (γ,n) cross section for ^{74}Ge. (b) The $(\gamma,2n)$ cross section for ^{74}Ge. (c) The total cross section $\sigma[(\gamma,n)+(\gamma,2n)+(\gamma,np)+(\gamma,p)]$ for ^{74}Ge.

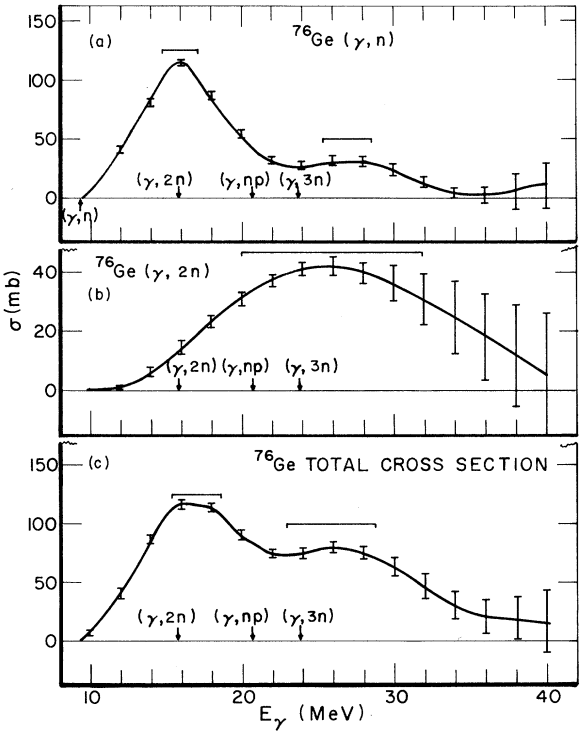

FIG. 7. (a) The (γ,n) cross section for ^{76}Ge. (b) The $(\gamma,2n)$ cross section for ^{76}Ge. (c) The total cross section $\sigma[(\gamma,n)+(\gamma,2n)+(\gamma,np)+(\gamma,p)]$ for ^{76}Ge.

places; near threshold energies, and above the giant dipole resonance. The neutron separation energy of ^{70}Ge is 11.5 MeV but the cross section remains positive to 10 MeV. The large negative dip centered at 26 MeV is clearly unphysical and is known to be associated with the unfolding procedure. A secondary structure correlated with this dip appears near 34 MeV but the reliability of the shape of the cross section at this energy is questionable. The single photoneutron cross section falls rapidly just above the $(\gamma, 2n)$ threshold. The $(\gamma, 2n)$ cross section is the smallest of all the $(\gamma, 2n)$ cross sections and appears with large uncertainties and in poor resolution. The curve begins to rise much before the $(\gamma, 2n)$ threshold. The cross section rises slowly until the maximum value of 5.2 mb is reached at 25 MeV, and appears to fall slowly at higher energy. The total cross section has the narrowest giant resonance of all the isotopes (<5.5 MeV). The peak cross section of 150 mb is at 16 MeV and the cross section at 34 MeV is 41 mb. Two previous measurements of the ^{70}Ge(γ, n) cross section have been reported; both were made by activation techniques using bremsstrahlung. Ferrero *et al.*[20] find a giant resonance at 18 MeV with a peak of 150 mb. Borello *et al.*[21] put the giant resonance at 20.5 MeV with a peak cross section of 125 mb. The high resonance energy obtained in this last measurement is probably due to the fact that the unfolding process was hampered by the lack of any yield data above 22 MeV.

2. ^{72}Ge

The ^{72}Ge(γ, n) cross section is obtained from the neutron counting measurement. As in the case of ^{70}Ge, the unphysical negative cross section above the giant resonance is an aberration associated with the statistical quality of the data. The structure at higher energy, near 35 MeV, cannot be defined with certainty.

The single neutron cross section rises slowly from threshold at 10.7 MeV and declines above the giant resonance at about 4 MeV above the $(\gamma, 2n)$ threshold. The $(\gamma, 2n)$ cross section starts up near threshold to a peak value of 30 mb near 27 MeV and then falls off slowly. The integrated $(\gamma, 2n)$ cross section for ^{72}Ge is seven times the integrated $(\gamma, 2n)$ result for ^{70}Ge. The total cross section has a giant resonance peak value of 140 mb at 17.5 MeV. No previous measurements have been reported.

3. ^{74}Ge

The ^{74}Ge(γ, n) cross section is a neutron counting result. A slight distortion of the cross section is seen near 10 MeV with a negative point, but the cross section rises steeply above the neutron separation energy. As in ^{72}Ge, the single neutron cross section is seen to decline about 4 MeV above the $(\gamma, 2n)$ threshold. The $(\gamma, 2n)$ cross section is not zero at threshold (due to poor resolution), rises slowly, and reaches a maximum value of 34 mb at about 23 MeV. The giant resonance has a larger width than in either ^{70}Ge or ^{72}Ge. The total cross section rises steeply to a peak value of 135 mb at about 16.5 MeV. The cross section falls slowly from the peak value at higher energies. As in the case of ^{72}Ge, no previous results have been reported in the literature.

4. ^{76}Ge

The ^{76}Ge(γ, n) result was obtained from the activation data, and has the least statistical error of all the data. The cross section at higher energy no longer has a resonant shape but is seen as a broad shoulder on the giant resonance. The single neutron cross section rises from threshold at the neutron separation energy, but has considerable strength well above the $(\gamma, 2n)$ threshold. The $(\gamma, 2n)$ cross section has poor resolution and appears to rise slowly several MeV below threshold. It reaches a maximum value of 42 mb near 26 MeV and begins to fall at higher energy. The integrated $(\gamma, 2n)$ cross section is the largest (710 MeV mb) of all four isotopes. This value is nearly 12 times the ^{70}Ge result.

The giant resonance of ^{76}Ge is the broadest of all four isotopes (>8 MeV). The total cross section has a large shoulder at 26 MeV, due mainly to the large $(\gamma, 2n)$ contribution.

The only previous measurement is reported by Borello, Goldenberg, and Santos,[21] who find a giant resonance peaking at 19 MeV with a maximum value of 249 mb. These results are seen to be in poor agreement with the values reported here.

V. DISCUSSION

A. Total cross sections and dynamic collective theory

In order to study the character of the total cross section data, we have fit the experimental cross sections with a single Lorentz line shape using a least squares fitting technique. To obtain a good fit to the giant resonance, the points used in the fit were only those below and in the giant resonance itself. This procedure not only provides accurate estimates of giant resonance width and peak energy, but also a consistent basis for estimating the amount of cross section that is present at energies above the giant dipole resonance. Table III summarizes the fitting results and presents the

TABLE III. Lorentz fit parameters and integrated cross sections for total cross sections.

Isotope	σ_0 (mb)	Γ (MeV)	E_0 (MeV)	σ_{LF} $(\frac{1}{2}\pi)\sigma_0\Gamma$ (MeV mb)	σ_{Int} (MeV mb)	$\sigma_{Int}-\sigma_{LF}$ (MeV mb)	$D=60\frac{NZ}{A}$ (MeV mb)	$\frac{\sigma_{Int}}{D}$	$\frac{\sigma_{Int}-\sigma_{LF}}{\sigma_{Int}}$
^{70}Ge	150	5.85	15.5	1380	1463	83	1040	1.41	0.06
^{72}Ge	150	5.90	17.9	1390	1690	300	1070	1.58	0.18
^{74}Ge	144	6.96	16.5	1580	1805	225	1090	1.66	0.12
^{76}Ge	120	8.20	16.7	1550	1892	342	1110	1.70	0.18

values for the integrated cross sections to 40 MeV. The table also includes the result predicted by the classical dipole sum rule, and the ratio of the experimental integrated sum to this sum rule result.

The increasing FWHM of the main giant resonance with increasing neutron excess is in qualitative agreement with predictions of the dynamic collective model. Addition of neutrons makes the nuclear surface "softer," strengthening the dipole-surface vibration coupling which splits the giant resonance into several components. These components appear as one broad resonance in poor-resolution experiments of this type. In terms of dynamic collective model (DCM) of spherical nuclei as discussed by Weber, Huber, and Greiner[22]

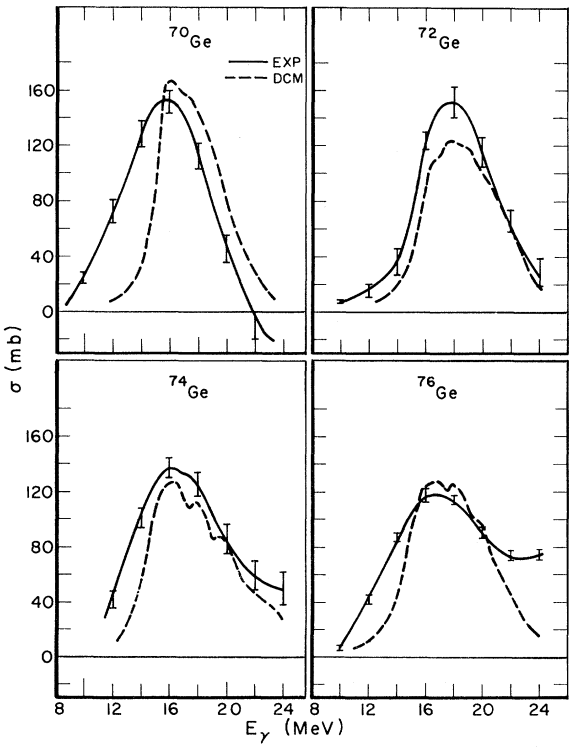

FIG. 8. Comparison of the measured photoabsorption cross sections with predictions of a dynamic collective model calculation using dipole matrix elements interpolated from the results of Huber *et al.* (Ref. 5).

and Huber *et al.*,[5] the germanium nuclei are particularly interesting. The characteristics of the low lying vibrational levels (β_0 = the measure of dynamic deformation, and E_2 = the energy of the first 2^+ state) enter into the DCM calculation and predict a large spreading of the main dipole state between ^{70}Ge and ^{76}Ge. The opportunity to compare these detailed model predictions with data from four adjacent isotopes has prompted us to calculate the germanium cross sections in the giant resonance region following the model of Huber *et al.*[5] This provides a check of the model predictions over a fairly wide range of β_0 and E_2 values. We have obtained values for the dipole matrix elements by interpolation of the results published by Huber *et al.*[5] The results of the calculations are presented and compared to the experimental cross sections in Fig. 8. In all cases, the calculations allow one dipole sum to be present in the giant resonance, and the width of individual Lorentzian levels that compose the dipole state is assumed to be 2 MeV. The energy of the unperturbed dipole state is chosen to fall at the peak energy of the Lorentz fit to the giant resonance.

The agreement between the calculated cross section and the experimental cross section is seen to be quite good. The measured cross sections have broad resonances, with the smallest width for ^{70}Ge, increasing widths for ^{72,74}Ge, and the largest width for ^{76}Ge. The width of the calculated cross sections follows this trend in good agreement over the isotopes. Good agreement is also obtained between the peak values and energy distribution of the main dipole strength for all four isotopes. It is unfortunate that the resolution of the experimental data does not allow a comparison of the finer details of the structure of the giant resonance.

The model calculations fail to explain the additional strength observed on the leading edge of the giant resonance, a failing that is known to be typical of this model. The discrepancy is most pronounced in ^{70}Ge, the "stiffest" nucleus of the four studied ($\beta_0 = 0.224$, $E_2 = 1.04$ MeV). Further, we observe that for all four nuclei the cross section has more strength at higher energies than can be accounted for in this model.

B. Cross section above the giant resonance

It is possible to make a reasonable estimate of the integrated cross section present above the giant resonance by employing the total integrated cross section, and the results of the Lorentz fitting procedure. Column 7 of Table III lists the difference between the experimental integrated cross section and the area under the fitted Lorentz line for each isotope. This difference represents the amount of integrated cross section above the giant resonance. Column 10 of Table III compares this amount to the total integrated cross section of each isotope. The average value of this ratio is about 0.14. Since the contribution of the (γ, p) and (γ, np) reactions to the total cross sections is quite small, the greatest contribution at energies above the giant resonance is from the (γ, n) and $(\gamma, 2n)$ reactions.

The existence and magnitude of a cross section at higher energy has been confirmed in investigations by groups at Livermore and Saclay. These groups have suggested that the electric quadrupole giant resonance and a direct neutron production contribution may be the source of the higher energy cross section. Recent electron scattering results[23-25] have reported broad resonance shapes in the cross section at about $120\,A^{-1/3}$ MeV in various nuclei, including Fe, Zr, and Pb. These structures have been classed as $E2$ in nature on the basis of form factor analysis, and thus lend support to photoabsorption results.

The electric quadrupole contribution to the photoabsorption cross section has been calculated by several authors. The simple hydrodynamic theory predicts a quadrupole resonance at 1.6 times the energy of the giant dipole resonance, or at 27 MeV for germanium. The integrated cross section of the quandrupole resonance is estimated to be about 8% of the integrated cross section of giant electric dipole resonance. On the basis of this discussion, we assume that a large fraction of the integrated cross section at higher energies for the germanium isotopes can be assigned to the electric quadrupole resonance. If we further assume a direct neutron production cross section that is consistent with estimates of the Saclay group, we can account for all the remaining integrated cross section above the giant dipole resonance.

VI. SUMMARY

We have obtained total photodisintegration cross sections for four isotopes of germanium from measurements of the cross section for (γ, n), $(\gamma, 2n)$, (γ, p), and (γ, np) reactions. We find that the peak cross section, energy, and width of the giant dipole resonance for each isotope can be reproduced in a qualitative manner by dynamic collective model calculations. In agreement with other measurements, we find considerable cross section on the rising side of the giant resonance that is not accounted for by the model calculation. While the cross section shape above the dipole resonance cannot be obtained from these data, the integrated cross section of each reaction has been measured with good precision. We estimate that 14% of the total integrated cross section appears above the giant resonance. Similar cross section strength has been reported by other groups which suggest that this strength is due to contributions from the electric quadrupole resonance, and direct neutron production. The present data for germanium are consistent with those assignments.

ACKNOWLEDGMENTS

The experimental data reported here were obtained in the last experiments performed at the Iowa State University Synchrotron Laboratory. In 20 years of active research, this laboratory has made many contributions to photonuclear reaction physics. A large part of the present work rests upon the firm support provided by the many people who have worked at the laboratory in the past years. The authors wish to acknowledge that effort at this time. One of the authors (J. J. McCarthy) wishes to thank Dr. Evans Hayward for helpful discussions.

---

*Present address: National Bureau of Standards, Nuclear Sciences Division, Washington, District of Columbia 20234.

†Present address: University of New Haven, Department of Physics, West Haven, Connecticut 06516.

‡Present address: U.S. Atomic Energy Commission, Directorate of Licensing, Washington, District of Columbia 20545.

[1]M. Danos and W. Greiner, Phys. Rev. 134, B284 (1964).

[2]J. Le Tourneux, Phys. Lett. 13, 325 (1964).

[3]S. F. Semenko, Phys. Lett. 10, 182 (1964); 13, 157 (1964).

[4]A. K. Kerman and H. K. Quang, Phys. Rev. 135, B883 (1964).

[5]M. G. Huber, M. Danos, H. J. Weber, and W. Greiner, Phys. Rev. 155, 1073 (1967).

[6]D. S. Fielder, J. Le Tourneux, K. Min, and W. D. Whitehead, Phys. Rev. Lett. 15, 33 (1965).

[7]J. S. Levinger, *Nuclear Photodisintegration* (Oxford U. P., New York, 1960).

[8]J. A. Carver, D. C. Peaslee, and R. B. Taylor, Phys.

Rev. 127, 2198 (1962).
[9]M. Danos, Ann. Phys. (Leipz.) 10, 265 (1952).
[10]R. Ligensa and W. Greiner, Nucl. Phys. A92, 673 (1967).
[11]R. L. Bramblett, J. T. Caldwell, R. R. Harvey, and S. C. Fultz, Phys. Rev. 133, B869 (1964); 129, 2723 (1963).
[12]R. Bergère, H. Beil, and A. Veyssiere, Nucl. Phys. A121, 463 (1968).
[13]A. DeVolpi and K. G. Porges, Phys. Rev. C 1, 683 (1970).
[14]D. W. Marquardt, J. Soc. Ind. Appl. Math. 11, 431 (1963).
[15]P. R. Bevington, *Data Reduction and Error Analysis for the Physical Sciences* (McGraw Hill, New York, 1969).
[16]B. I. Goryachev, At. Energ. 12, 246 (1962).
[17]B. C. Cook, Nucl. Instrum. Methods 24, 256 (1963).
[18]E. Bramanis, T. K. Deague, R. S. Hicks, R. J. Hughes, E. G. Muirherd, R. H. Sambell, and R. J. J. Stewart, Nucl. Instrum. Methods 100, 59 (1972).
[19]J. J. McCarthy, R. C. Morrison, and H. J. Vander Molen, Nucl. Phys. A213, 371 (1973).
[20]F. Ferrero, S. Ferroni, R. Malvano, S. Menardi, and E. S. Lua, Nucl. Phys. 15, 436 (1960).
[21]O. A. Borello, J. Goldenberg, and M. D. S. Santos, Am. Acad. Brasil. Cienc. 27, 413 (1955).
[22]H. J. Weber, M. G. Huber, and W. Greiner, Z. Phys. 192, 182 (1966).
[23]F. Dreyer, H. Dahmen, J. Staude, and H. H. Thies, Nucl. Phys. A192, 433 (1972).
[24]S. Fukuda and Y. Torizuka, Phys. Rev. Lett. 29, 1109 (1972).
[25]M. Nagao and Y. Torizuka, Phys. Rev. Lett. 30, 1068 (1973).
[26]E. G. Fuller, H. M. Gerstenberg, H. Vander Molen, and T. C. Dunn, *Photonuclear Reaction Data, 1973*, NBS Special Publication No. 380, March, 1973.